SEMARAK ILMU PUBLISHING

Journal of Advanced Research in Fluid Mechanics and Thermal Sciences

Journal homepage:
https://semarakilmu.com.my/journals/index.php/fluid_mechanics_thermal_sciences/index
ISSN: 2289-7879

Numerical Simulation of High-Speed Rotor for Air-cooled Eddy Current Dynamometer

Yew Heng Teoh[1,*], Ju Joe Lim Lau[1], Heoy Geok How[2], Jun Sheng Teh[1], Kok Hwa Yu[1], Horizon Gitano Briggs[3]

[1] School of Mechanical Engineering, Engineering Campus, Universiti Sains Malaysia, Nibong Tebal 14300, Penang, Malaysia
[2] Department of Engineering, School of Engineering, Computing and Built Environment, UOW Malaysia KDU Penang University College, 32, Jalan Anson, 10400 Georgetown, Penang, Malaysia
[3] Focus Applied Technologies Sdn. Bhd., Lot 463, Jalan Relau K134, Sungai Kechil Ilir, 14300 Nibong Tebal, Pulau Pinang, Malaysia

ARTICLE INFO

Article history:
Received 16 February 2022
Received in revised form 8 May 2022
Accepted 15 May 2022
Available online 12 June 2022

Keywords:
Rotor; airflow; temperature; dynamometer

ABSTRACT

The key feature of air-cooled dynamometer is the geometry of the rotor, which played a vital role in effective heat rejection. Dual application is limited for air cooled eddy current dynamometer due to excessive heat generation when the operating speed is up to a certain range. The aim of this research is to observe the air flow pattern and temperature distribution on the rotor of the air-cooled dynamometer with different geometry designs. In addition, the air flow and heat transfer simulation were carried out by using ANSYS software. Besides, the setting of normal size mesh was proposed in all design cases to reduce the computational time and the mesh files size of the simulation. Furthermore, a total of four configurations of rotating domain were designed and created using SolidWorks software, with each one differentiated with the features of holes and cover. The results of air flow velocity contour were compared with those of without the cover and holes on the rotor design. The optimum design in air motion distributed within all cases of numerical simulation were then observed and compared. To validate the simulation setup, experimental data were used to validate the airflow and heat transfer coupling simulation models. The results revealed that an improvement with more air volume movement can be observed at medium range and high velocity range for all models with cover features over the models without cover. Besides, the results also shows that the influences of hole features on air flow velocity were less significant as compared to the one with cover features. Also, the rotor design with cover and without holes were found to be the best configuration as it allows the as high as 27.7% greater air flow dynamic to achieved lowest steady state temperature as compared with those of baseline design. The Design C also improved in term of temperature as compared to the simple model of plane rotor, with as high as 11.6% reduction in overall temperature. Through the results of this analysis, it was justifiable that the Design C can be suggested as the best-case scenario for further experimental study. These results will serve as a basis for rotor design to improve the performance of the air-cooled eddy current dynamometer.

* *Corresponding author.*
E-mail address: yewhengteoh@usm.my

https://doi.org/10.37934/arfmts.96.1.153167

1. Introduction

A dynamometer is an instrument for applying a controllable load to a mechanical power source (engine or motor) and measuring the speed and torque, thus the power [10]. While there are many kinds of dynamometers available, the least expensive type is the "Air Cooled Eddy Current Retarder" type [11]. Typically, an air-cooled eddy current retarder incorporates large diameter centrifugal fans integrated into their rotors to help expel heat generated via breaking action, as shown in Figure 1 [13]. Water cooled versions also exist, however these are much more expensive as they require careful sealing, and a water circulation system to pull away the generated heat, as shown in Figure 2 [6]. Air cooled units tend to be somewhat larger, and thus have a lower maximum speed limit (typically 4000 - 5000 rpm) than the equivalent power water cooled units, which can spin up to 6000 - 8000 rpm typically. Besides, dynamometers can be connected directly to the engine or motor being tested (thus called an Engine Dynamometer), or the dynamometer can be connected to large rollers which are driven by a vehicle's wheels [4]. In this configuration it is referred to as a Chassis Dynamometer. The retarder in a chassis dynamometer generally spins at lower speeds (1000 - 4000 rpm), thus this segment is dominated by air-cooled eddy current retarders. Most chassis dynamometers use the air-cooled eddy current retarders due to their lower cost and lower heat generation [1]. Some low-speed diesel engine dynamometers can use air cooled eddy current dynamometers, however for testing higher speed engines such as petrol engines generally water-cooled units are used due to excessive heat generation, but the equipment is much more expensive than an air-cooled type. Engine dynamometers also commonly used to investigate the engine power and emission characteristics for engine operation with biodiesel and its blends [5,15-18].

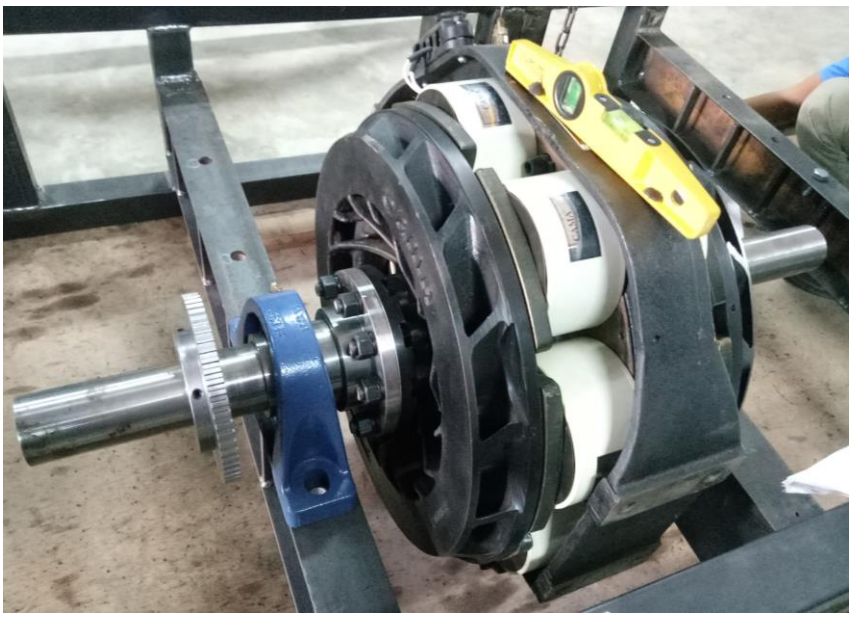

Fig. 1. Air-Cooled Retarder

Fig. 2. Water-Cooled Retarder

The basic problem is that the air-cooled units incorporate a large fan cast into the rotors. The rotors are thus produced out of cast iron in large diameters, which limits their maximum speed due to their material and design characteristics. But rotors made from high strength steel billets could be spun at higher speeds (e.g., 8,000 rpm). Even though price will increase steeply using high strength steel rotors but allows for high speed direct-engine applications for both engine and vehicle testing. Currently, the market has one suitable product for one application but lacks a product which can satisfy both the demands (engine and vehicle testing) with one product (considering the concept of one-size-fit-all). From the previous works, it is evident that most of the studies have been focused on the design and fabrication of eddy current dynamometer [11,12]. In fact, the operation of an air-cooled eddy current dynamometer involves a few physics, including magnetic and electric fields, and its performance is closely linked to heat transfer and air flow physics. Thus, a research gap remains in these fields which are addressed in this research study. The outcome due to the changes in fin cover design and optimization of an aerodynamically efficient vents for rotor cooling will be investigated in the present study. The airflow and heat transfer simulation are carried out using ANSYS. From the results, the effect of each fin cover design will be determined to enhance the air flow via the rotor fins and improve the heat dissipation.

2. Methodology

In the operation of Eddy Current dynamometer, the heat is generated on the rotor due to electromagnetic heating and speed-energy (kinetic energy) [2,19]. Typically, the rise in temperature will cause the low-performance problem for dynamometer [8,9]. The heat transfer simulations are proposed to estimate the temperature distribution [7]. Computational fluid dynamic simulations are proposed to optimize the rotor shape for air cooling purposes [2]. Besides being a conductor, it also acts as a cooling fan. The airflow coupled with the heat transfer simulation were considered in this study. Cooling can be achieved by driving air through the heated system. The cooling effect is investigated by observing the influence on temperature distribution by varying the rotor design. The version of ANSYS used is Academic 19.2. The license is for research and can support huge models. To solve the fluids flow and heat transfer problem numerically, ANSYS Structural; Thermal analysis and ANSYS Fluent; fluid flow is used. The air flow velocity around the rotor and temperature distribution on the conductor is estimated. The modelling process in ANSYS is illustrated in the flow diagram in

Figure 3. As shown in Figure 4 is the model consists of a shaft and a rotor. The rotor outer diameter is 370mm, the inner diameter is 50mm, and the rotor material is made of low carbon steel 1020 [3,14].

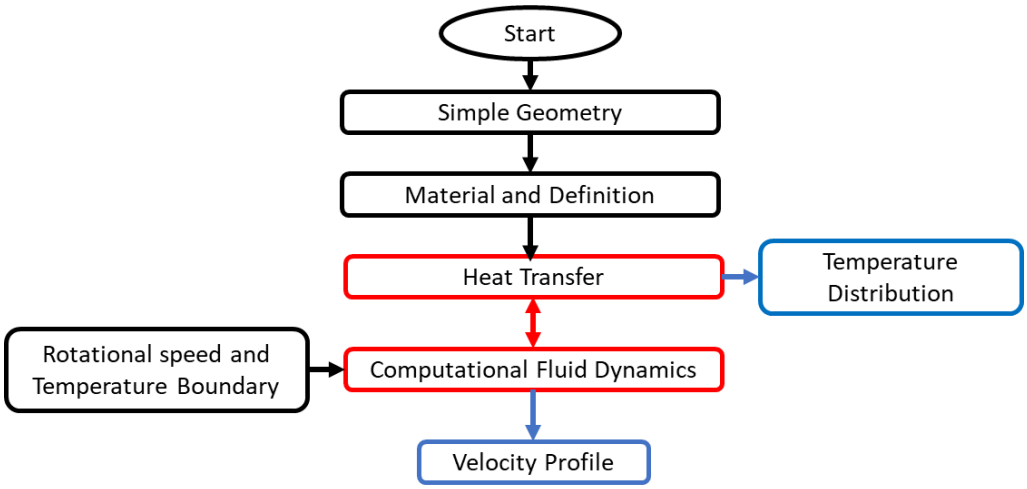

Fig. 3. Process flow of fluid flow and heat transfer simulation using ANSYS

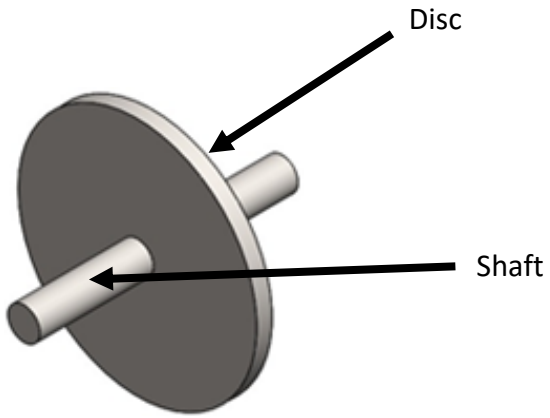

Fig. 4. Geometry created using SOLIDWORK

Assumption was made for 160kW of air-cooled eddy current dynamometer, that each rotor absorbs 80kW of power (i.e., the dynamometer consisted of 2 rotors, with each at front and back end). As the volume of the rotor is known, heat generation is calculated as 0.024105254 W/mm^3. Convections are applied on all outer surfaces of the rotor and shaft no to the end, defined with film coefficient, 7.9e-6 W/mm^2. All the faces of the model that contact to air are set to be radiating to ambient temperature of 295.15K, where emissivity is 0.3. Furthermore, the fluid-solid interface boundary condition is applied to the fluid facing surface of the rotor. These interfaces are created for temperature data transferring and receiving purposes.

For the portion of setting up in ANSYS Fluent, the k-epsilon (k-ε) turbulence model is used due to its good convergence rate and relatively low memory requirements. Assembly is set for the pressure outlet. The working fluid for this model is air. The rotor surface is set as a wall boundary as illustrated in Figure 5. Rotor was defined as a moving wall rotating at z-axis with 8000rpm. Its heat transfer option is set to system coupling. At the material name, mild steel is chosen.

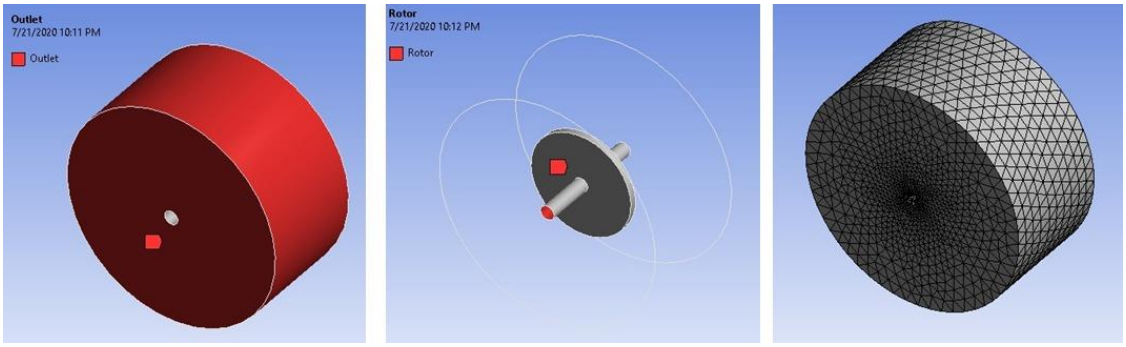

(a) (b) (c)

Fig. 5. (a) Defined boundary outer surface of air as outlets, (b) defined rotor surface as rotor wall, (c) fluid(air) meshing

The cases are a coupled problem of fluid flow and heat transfer. Thus, three system in ANSYS were used, Thermal analyses, Fluent, and System coupling. State thermal system is needed to describe the temperature of the rotating rotor and the fluid flow system that uses the fluent solver is needed to describe the temperature of the moving fluid as well. System coupling is needed to transfer temperature data from the mechanical system to the fluid system vice versa. Note that this is a two-way data transfer method. The sources and recipient of the data transfer is rotor and fluid-solid interface.

One of the most critical steps in the finite element method is to generate a good mesh. This is because, defective mesh may misrepresentation of the problem, which resulting unreliable results. To check the effect of grid resolution on accuracy of numerical results. Two types of mesh were considered, namely normal and fine. Table 1 shows the simulation results comparison between normal mesh and refined one. Since the percentage of error of the normal mesh compared to the refined one is insignificant as compared with the number of elements. Therefore, normal size mesh is proposed to use to perform in all case to reduce the computational time and the mesh files size of the simulation. Figure 6 shows the temperature distribution of color in contour scale on the rotor for different size of meshes model.

Table 1
Simulation results in term of maximum and minimum temperature for normal and refine mesh rotor

Mesh type	Nodes	Elements	Maximum Temperature	Minimum Temperature
Refined mesh	105,859	22,384	2,003.5	862.6
Normal mesh	32,463	6,956	2,003.5	862.9

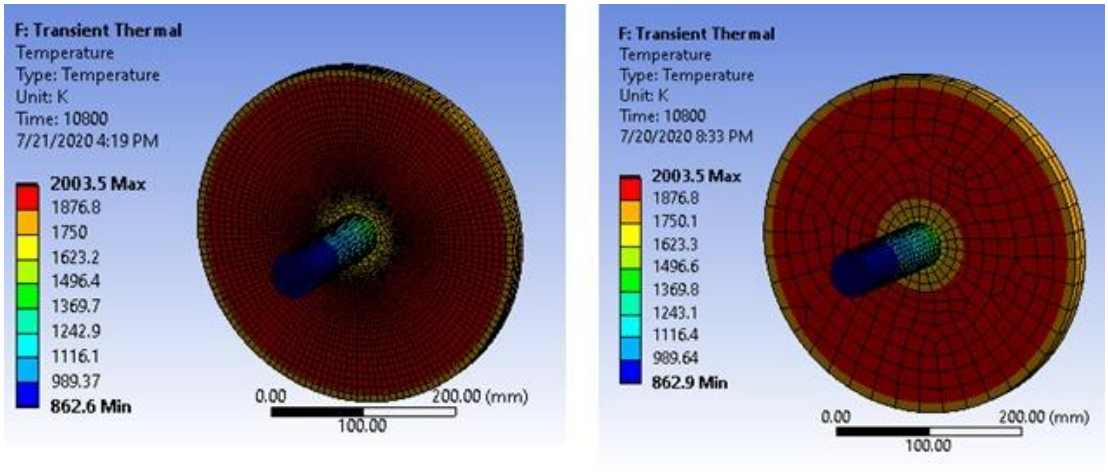

(a) (b)

Fig. 6. Temperature distribution on rotor for (a) refined mesh and (b) normal mesh model

To study the rotor performance in term of air flow velocity in open air conditions, two domains must be created which are the rotating domain and stationary domain. The rotating domain represents the rotor model, while the stationary one represents the environment flow around the rotor. In this study, the air was selected as a working fluid. Besides, SolidWorks software was adopted in this study to design the difference structure of the rotor and create the stationary and rotating domain as shown in Figure 7 and the detail of mesh is shown in Table 2. Four configurations of rotating domain have been designed and created, each one differentiated with the features of holes and cover as illustrated in Figure 8.

Table 2
Details of mesh

Display	Display Style	Use Geometry Setting
Defaults	Physics Preference	CFD
	Solver Preference	Fluent
	Element Order	Linear
	Element Size	60.0 mm
	Export Format	Standard
Sizing	Growth Rate	1.2
	Max. Size	120.0 mm
	Mesh Defeaturing	Yes
	Defeature Size	0.3 mm
	Capture Curvature	Yes
	Curvature Min Size	0.6 mm
	Curvature Normal Angle	18.0°
	Size Formulation (Beta)	Program Controlled
	Bounding Box Diagonal	1200.0 mm
	Average Surface Area	2.8254e+005 mm^2
	Minimum Edge Length	125.66 mm
Quality	Check Mesh Quality	Yes, Errors
	Target Skewness	0.900000
	Smoothing	High

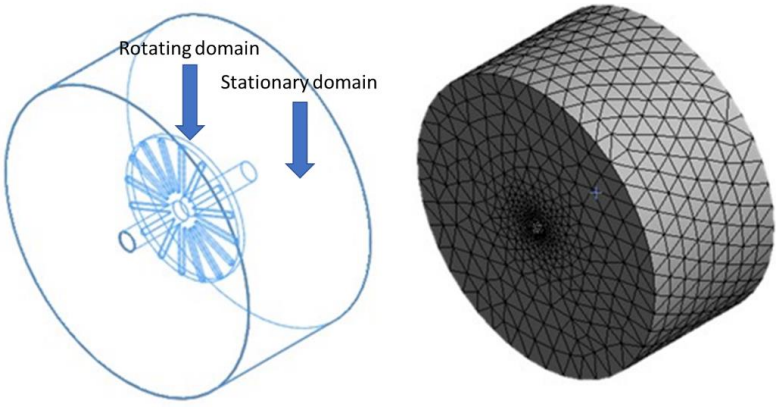

Fig. 7. (a) Defined model domains and (b) Entire mesh model

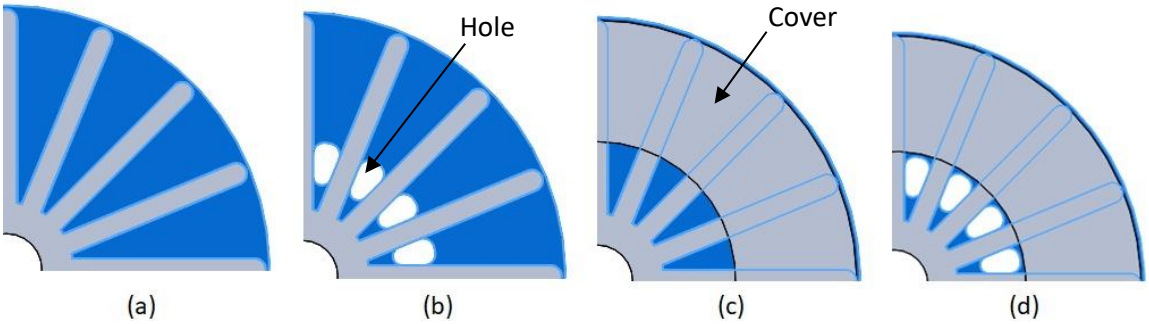

Fig. 8. Various structure of rotors, (a) without hole and cover, (b) with hole and without cover, (c) without hole and with cover, and (d) with hole and cover

ANSYS Fluent software was used in this study to analyse air flow velocity on surrounding air. Transient air flow simulation is performed. General model and boundary conditions are setting up as aforementioned. Changing of steady state solver to transient solver is necessary when setting up the general model. For solve method, retain the default solution methods for flow. Under solving controls, active the pseudo transient method then retain the default solution controls. In this study, a total of 200 iterations were adopted to obtains the first 20 s results.

3. Results and Discussions

3.1 Experimental Validation of a Simulation Model

To prove that the simulation setup is valid. Experimental data are used for the validation of airflow and heat transfer coupling simulation models. The experiment is conducted twice, first test is conducted with a plane rotor while second test is conducted with plane rotor attached with straight fin cover as illustrated in Figure 9. In the testing, rotor was rotating constantly with the range of speed 1000-1100 rpm, 35Nm for 25 minutes, followed by 45Nm for 5 minutes, then no load for several minutes. Figure 10 shows the whole experimental setup of the second test, plane rotor is attached with straight fin cover.

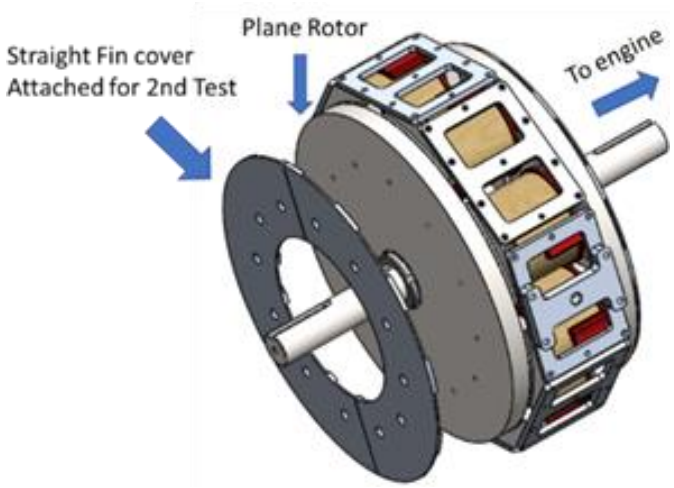

Fig. 9. Simulation models for two tests

Fig. 10. Experimental setup for second test

The experimental outcomes are rotor temperatures, $Temp_{in}$ and $Temp_{out}$ is measured and recorded. $Temp_{in}$ refer to temp. near center shaft while $Temp_{out}$ refer to temperature near outer rotor. Average temperatures are calculated between them, and the experimental results are shown in Figure 11. These outcomes will then compare with the simulation outcomes for the same models. The simulation model is modelled by using ANSYS software and the CAD file is created using SolidWorks. To better define the mesh, the CAD is transformed into a simplified form by removing the small hole on the parts and connections between parts like screws. The rotor peak temperature for both experimental and simulation under 2 different torque settings of 35Nm and 45Nm, as well as with 2 different rotor designs are tabulated in Table 3. As can be seen, the peak temperature identified from the simulation model are in an acceptable range as compared to those of experimental data and with an average difference of 6%, hence identical setup of simulation for differences models are proceeded.

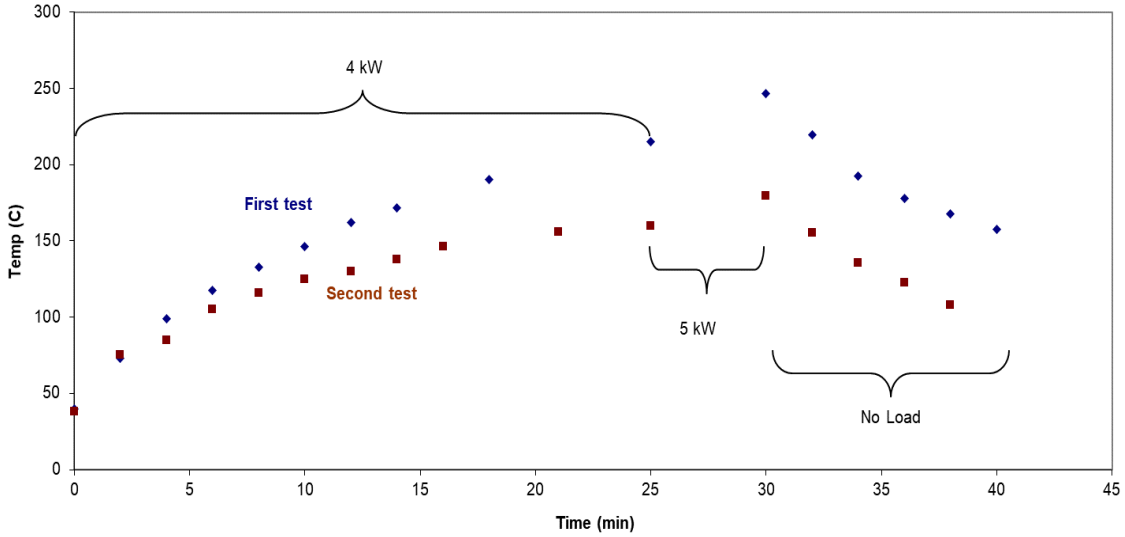

Fig. 11. Experimental results for two tests series

Table 3
Peak temperature results for both experimental and the simulation tested under various torque and rotor designs

Configuration	Torque (Nm)	Peak Temperature, °C		% Difference
		Experimental	Simulation	
Plane Rotor (without cover)	35	190.0	187.2	-1.5
	45	246.5	224.6	-8.9
Plane Rotor with Straight Fin Cover	35	138.0	126.8	-8.1
	45	160.0	150.9	-5.7

3.2 Effect of Rotor Design on Air flow and Temperature Distribution

Optimal selection of rotor shape design is important for air cooling purposes in the system. Various designs of rotor as shown in Figure 12 were considered to perform airflow and thermal analysis with differences configuration. The Design A, B, C and D were undergoing airflow analysis to identify the right features of the rotor to drive more air to move. As a result, the feature of cover increases the average value of airflow velocity, while the features of hole reduce the average value of airflow velocity of the system [21]. Therefore, the Design C which designed with the cover and without the hole features having better airflow results among these cases. The air flow pattern and velocity change with various rotor designs can be seen in Table 4. As can be observed, the air flow velocity profile around the rotor is vary significantly for the respective model with differences features. In fact, the multiplication between percentages of volume of air domain and its velocity was also calculated and tabulated in this table. As shown in Figure 13 is the results of percentages of volume of air domains and total volume times velocity versus velocity graph for varies rotor designs. As can be seen, the Design A was marked as the baseline of the model and comparison were made between this and another.

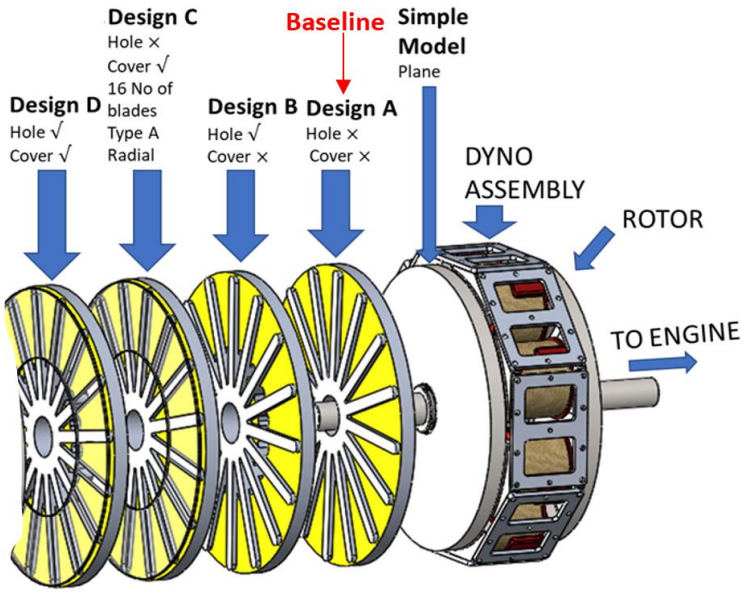

Fig. 12. All design models modelled and studied in this study

Table 4
Air flow velocity profile around the rotor and the multiplication between percentages of volume of air domain and its velocity for respective model with differences features.

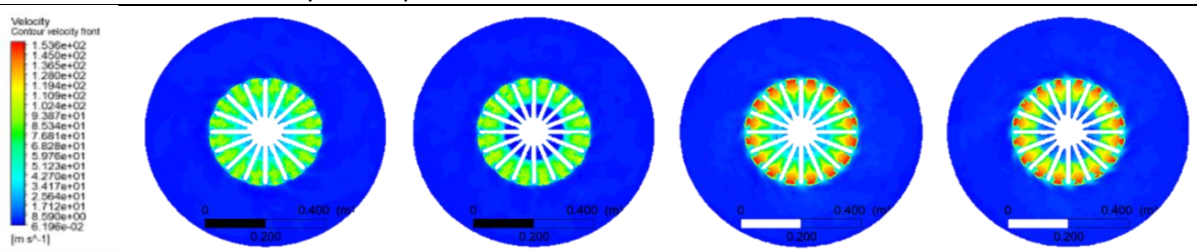

Design	A (Baseline)	B	C	D
Hole	X	✓	X	✓
Cover	X	X	✓	✓
(Velocity) x (%volume)	142.8	135.5	182.3	154.8
%Difference vs. Design A	0	-5.1%	+27.7%	+8.4%

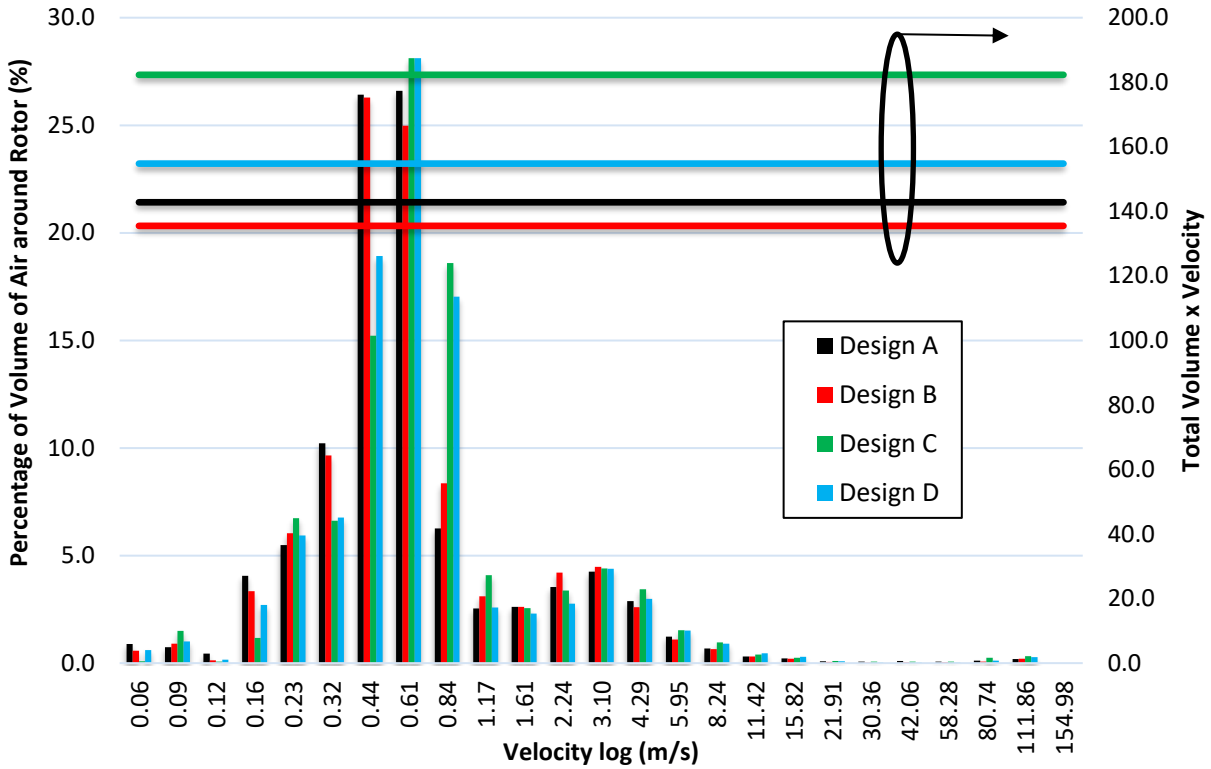

Fig. 13. Percentages of volume of air domains and total volume times velocity versus velocity graph for varies rotor designs

Accordingly, the total average air flow velocity of the Design C was the higher among all, which follows by the Design D, Design A and the lowest, Design B. The comparison of air flow velocity in the case of the differences attached features such as hole and cover allowed the concluding that the feature of cover increase the average value of air flow velocity and the feature of hole reduces the average value of air flow velocity of the system. As the rotor requires torque to keep the rotational motion, hence the mechanical power consumption is dependent on the magnitude of torque. In addition, the range of motion on the system can be operated smoothly when the system's air flow velocity reduces, thus the rotor's torque drops as well. The uniform-wall-temperature rotor plates transmit heat into the system by raising the air temperature above the entrance temperature. As a result, the temperature of the system may be decreased. Therefore, the Design C which designed with the cover and without the hole features having a better ai flow results among all the cases.

The air flow velocity was classified in three classes which are low (0.06 to 0.84 m/s), medium (0.84 to 11.42 m/s) and high (11.42 to 154.98 m/s) and plotted in graph according to its models as illustrated in Figure 14. As can be seen, larger portion of air which above 50% are at low velocity range across all models. Improvement with more air volume moving can be observed at medium range and high velocity range for all models with cover features over the models without rotors. The influences of hole features on effect of air flow velocity were less significant compared to the cover features.

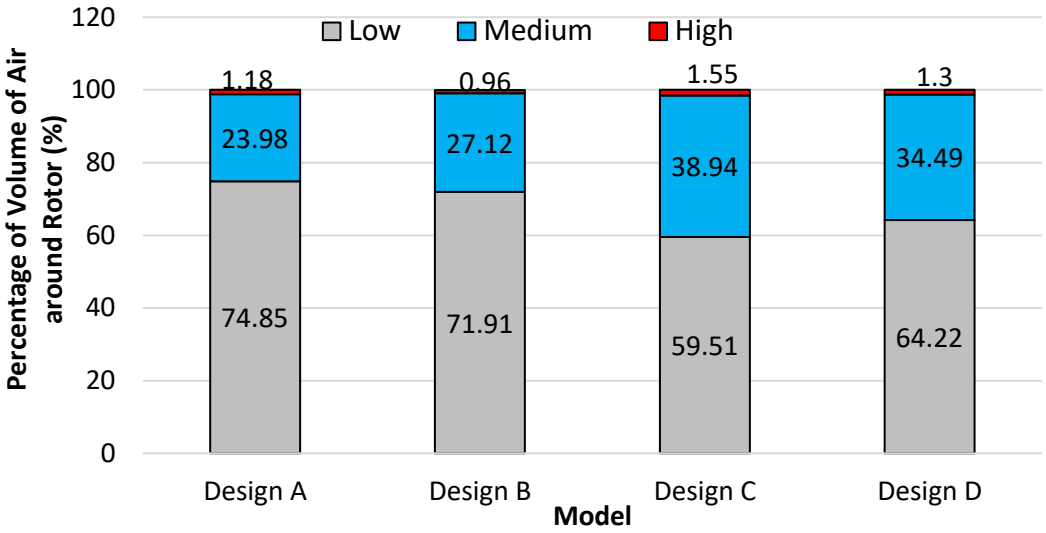

Fig. 14. Air velocity range distribution for differences structure of rotor

In this study, the simulation of thermal analysis was performed by comparing the simple model (refer Figure 12) and the conceptual model. The conceptual model of the Design C was selected based on the previous results of air flow analysis. It was constructed with a proper feature to allow for driving more air movement. This comparison is essential to prove that the Design C of the rotor with fins and cover could produce a better performance in heat rejection. This comparative study of thermal analysis simulation is by comparing in terms of temperature distribution. For a fair comparison of average temperature of the rotor, plane A was created, which locate at the center of cross-section of the rotor as illustrated in Figure 15. The temperature distribution of colour in contour scale on the plane A for simple model and the Design C were illustrated in Figure 16. To provide a better indication of total temperature under different air flow condition, the multiplication between percentages of plane area and its temperature was calculated and plotted in Figure 17.

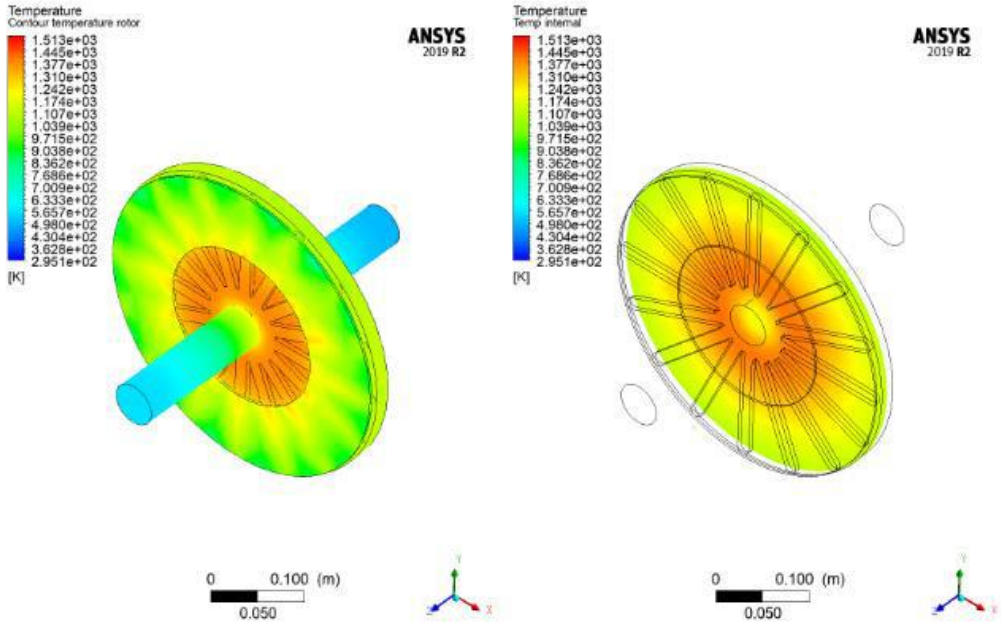

(a) (b)

Fig. 15. (a) Temperature distributed on rotor and (b) temperature distributed on plane A

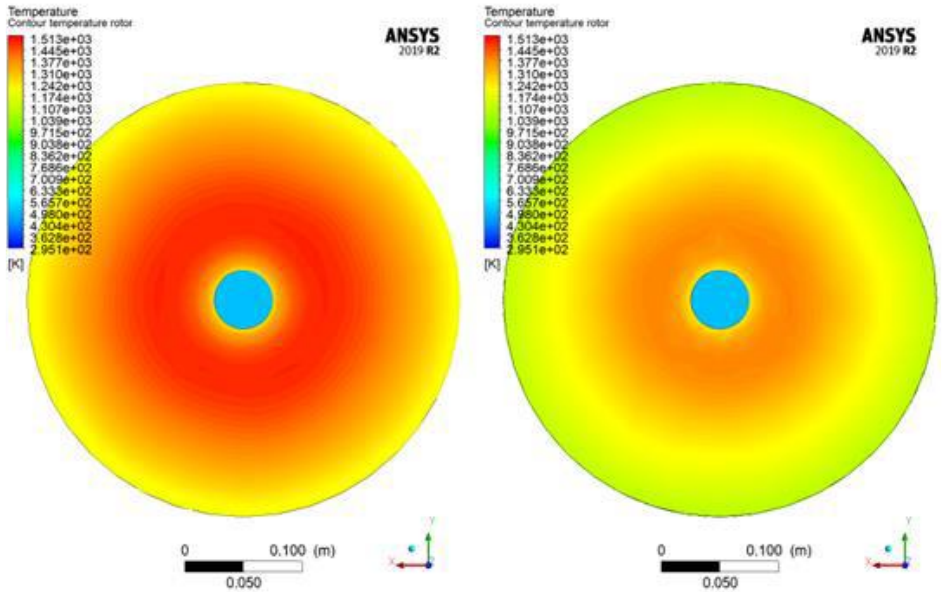

Fig. 16. Temperature distribution profile on plane A for (a) simple model and (b) the Design C

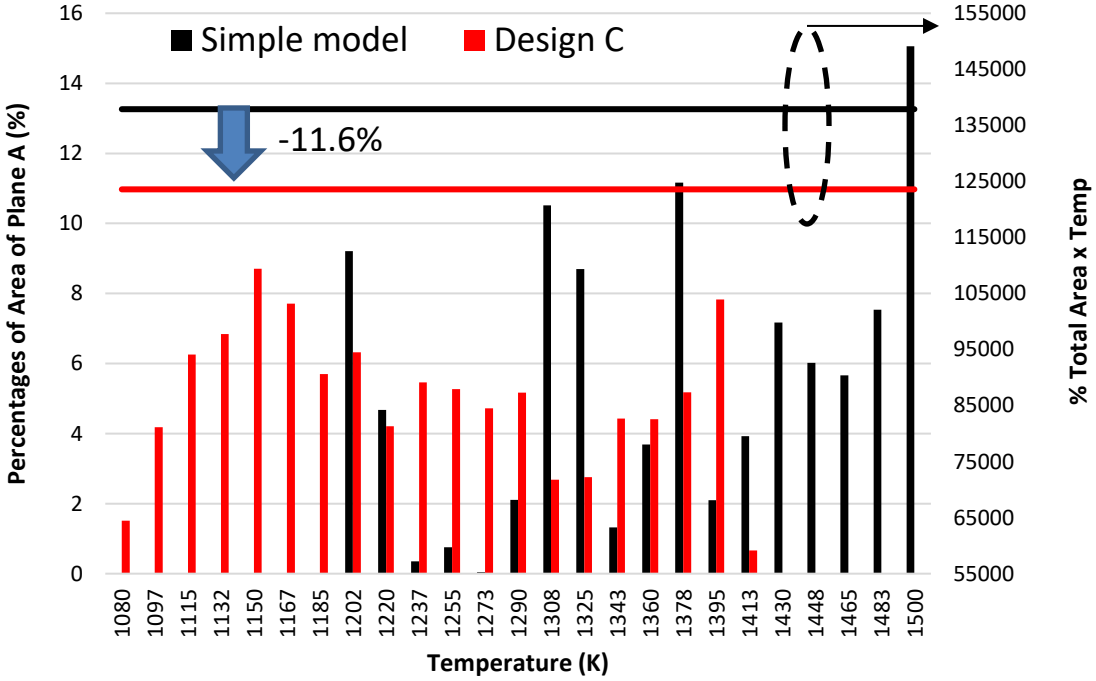

Fig. 17. Percentages of area of plane A and total area times temperature versus temperature graph for simple model and conceptual model

According to the results presented in Figure 17, it was noticed that the Design C improved in term of temperature as compared to the simple model of plane rotor. The percentages of reduction in total temperature (i.e., %Total Area x Temp.) were calculated as 11.6% as compared to the simple model. When the dynamometer is running at a constant speed, an increase in temperature induces an increase in the rotor phase eddy current. As the percentages of total temperature drop fall, the dynamometer's efficiency will be increased under a constant speed condition. Through the results of this analysis, it was justifiable that the Design C can be suggested as the best-case scenario for further experimental study.

4. Conclusions

From the results of the study, the rotor design has a significant impact on the flow velocity. By comparing the results, it was discovered that the greater the average air flow velocity around the rotor, the lower the rotor temperature can be achieved. Furthermore, design C has achieved the best results with the higher air flow velocity and lower temperature. As a result, we can conclude that the cover features have improved the flow velocity of the air surrounding the rotor. Recommendations for future research is to study the effects of curvature blade angle, blade length, and rotor blade depth on airflow velocity and rotor temperature.

Acknowledgement
The authors would like to acknowledge the Ministry of Higher Education of Malaysia, Universiti Sains Malaysia and Focus Applied Technologies Sdn. Bhd. for the support through Public-Private Research Network (PPRN)- 304.PMEKANIK.6314055 (Title: Design and Development of High Speed Rotor For Air-Cooled Eddy Current Dynamometer).

References

[1] Arseneau, Paul. "Chassis dynamometer having an eddy current brake with adjustable air gap and modular components." *U.S. Patent 8,015,863*, issued September 13, 2011.
[2] Baktash, Iman. "Modeling of Electromagnetic Heating of Multi-coil Inductors in Railway Traction Systems." *Master's thesis, Blekinge Institute of Technology* (2015).
[3] Costa, Leonardo F. T., Marcos F. de Campos, Gunther J. L. Gerhardt, and Frank P. Missell. "Hysteresis and Magnetic Barkhausen Noise for SAE 1020 and 1045 Steels With Different Microstructures." *IEEE Transactions on Magnetics* 50, No. 4 (2014): 1-4. https://doi.org/10.1109/TMAG.2013.2287701
[4] Herling, R. J. *Development of specifications for a motorcycle dynamometer and motorcycle cooling system. Volume II*. Specifications. Final report Sep 74--Feb 76. No. PB-253266. Olson Labs., Inc., Anaheim, CA (USA), 1976.
[5] How, H. G., Y. H. Teoh, B. Navaneetha Krishnan, T. D. Le, H. T. Nguyen, and C. Prabhu. "Prediction of optimum Palm Oil Methyl Ester fuel blend for compression ignition engine using Response Surface Methodology." *Energy* 234 (2021): 121238. https://doi.org/10.1016/j.energy.2021.121238
[6] Jaeschke, Ralph L. "Fluid-cooled dynamometer." *U.S. Patent 3,863,083*, issued January 28, 1975.
[7] Aslfattahi, Navid, Alireza Zendehboudi, Saidur Rahman, Mohd Faizul Mohd Sabri, Suhana Mohd Said, A. Arifutzzaman, and Nor Azwadi Che Sidik. "Optimization of thermal conductivity of NanoPCM-based graphene by response surface methodology." *Journal of Advanced Research in Fluid Mechanics and Thermal Sciences* 75, no. 3 (2020): 108-125. https://doi.org/10.37934/arfmts.75.3.108125
[8] Korm, Kevin. "Air-cooled brake rotor system." *U.S. Patent Application 11/350,531*, filed August 9, 2007.
[9] Lubin, Thierry, Smail Mezani, and Abderrezak Rezzoug. "Experimental and theoretical analyses of axial magnetic coupling under steady-state and transient operations." *IEEE Transactions on Industrial Electronics* 61, no. 8 (2013): 4356-4365. https://doi.org/10.1109/TIE.2013.2266087
[10] Martyr, Anthony J., and Michael Alexander Plint. *Engine testing: theory and practice*. Elsevier, 2011.
[11] Mate, Nilesh R., and D. Y. Dhande. "A Study of the Two Wheeler Retarder Type Dynamometer System." *International Journal of Innovative Research in Science, Engineering and Technology* 3, no. 2 (2014): 9057-9061.
[12] Sinaga, Nazaruddin. "Numerical simulation of the width and angle of the rotor blade on the air flow rate of a 350 kW air-cooled eddy current dynamometer." In *Journal of Physics: Conference Series*, vol. 1373, no. 1, p. 012021. IOP Publishing, 2019. https://doi.org/10.1088/1742-6596/1373/1/012021
[13] Staats, Wayne L., and John G. Brisson. "Active heat transfer enhancement in air cooled heat sinks using integrated centrifugal fans." *International Journal of Heat and Mass Transfer* 82 (2015): 189-205. https://doi.org/10.1016/j.ijheatmasstransfer.2014.10.075
[14] Takeuchi, Hirohisa, Yasuhiro Yogo, Tsuyoshi Hattori, Tomonori Tajima, and Takashi Ishikawa. "High-temperature magnetization characteristics of steels." *ISIJ International* 57, no. 10 (2017): 1883-1886. https://doi.org/10.2355/isijinternational.ISIJINT-2017-145
[15] Teoh, Yew Heng, Heoy Geok How, Navaneetha Krishnan Balakrishnan, Thanh Danh Le, and Huu Tho Nguyen. "Performance, Emissions, Combustion and Vibration Analysis of a CI Engine Fueled with Coconut and Used Palm Cooking Oil Methyl Ester." *Processes* 8, no. 8 (2020): 990. https://doi.org/10.3390/pr8080990

[16] Teoh, Yew Heng, Heoy Geok How, Thanh Danh Le, and Huu Tho Nguyen. "Alexandrian Laurel for biodiesel production and its biodiesel blends on performance, emission and combustion characteristics in common-rail diesel engine." *Processes* 8, no. 9 (2020): 1141. https://doi.org/10.3390/pr8091141

[17] Teoh, Yew Heng, Heoy Geok How, Farooq Sher, Thanh Danh Le, Huu Tho Nguyen, and Haseeb Yaqoob. "Fuel injection responses and particulate emissions of a CRDI engine fueled with cocos nucifera biodiesel." *Sustainability* 13, no. 9 (2021): 4930. https://doi.org/10.3390/su13094930

[18] Teoh, Yew Heng, Heoy Geok How, Farooq Sher, Thanh Danh Le, Hwai Chyuan Ong, Huu Tho Nguyen, and Haseeb Yaqoob. "Optimization of fuel injection parameters of moringa oleifera biodiesel-diesel blend for engine-out-responses improvements." *Symmetry* 13, no. 6 (2021): 982. https://doi.org/10.3390/sym13060982

[19] Van Mierlo, Joeri, Gaston Maggetto, Erik Van de Burgwal, and Raymond Gense. "Driving style and traffic measures-influence on vehicle emissions and fuel consumption." *Proceedings of the Institution of Mechanical Engineers, Part D: Journal of Automobile Engineering* 218, no. 1 (2004): 43-50. https://doi.org/10.1243/095440704322829155

[20] Yang, Zhuo, Baoqing Deng, Mengqi Deng, and Shaojia Huang. "An overview of chassis dynamometer in the testing of vehicle emission." In *MATEC Web of Conferences*, vol. 175. EDP Sciences, 2018. https://doi.org/10.1051/matecconf/201817502015

[21] Kee, Tristan Yeo Eng, Chong Kok Hing, Basil Wong Tong Liong, Victor Bong Nee Shin, Lee Man Djun, and Christopher Jantai Anak Boniface. "Alternative Design of Air Ventilation in Passenger Lift for Thermal Comfort." *CFD Letters* 12, no. 1 (2020): 37-47.